Journal of Biomedical Optics

SPIEDigitalLibrary.org/jbo

Label-free *in vivo* imaging of human leukocytes using two-photon excited endogenous fluorescence

Yan Zeng
Bo Yan
Qiqi Sun
Seng Khoon Teh
Wei Zhang
Zilong Wen
Jianan Y. Qu

SPIE

Label-free *in vivo* imaging of human leukocytes using two-photon excited endogenous fluorescence

Yan Zeng,[a] Bo Yan,[b] Qiqi Sun,[a] Seng Khoon Teh,[a] Wei Zhang,[a] Zilong Wen,[b,c] and Jianan Y. Qu[a,c]
[a]Hong Kong University of Science and Technology, Department of Electronic and Computer Engineering, Biophotonics Research Laboratory, Clear Water Bay, Kowloon, Hong Kong SAR, China
[b]Hong Kong University of Science and Technology, Division of Life Science, State Key Laboratory of Molecular Neuroscience, Clear Water Bay, Kowloon, Hong Kong SAR, China
[c]Hong Kong University of Science and Technology, School of Science and Institute for Advanced Study, Center of Systems Biology and Human Health, Clear Water Bay, Kowloon, Hong Kong SAR, China

Abstract. We demonstrate that two-photon excited endogenous fluorescence enables label-free morphological and functional imaging of various human blood cells. Specifically, we achieved distinctive morphological contrast to visualize morphology of important leukocytes, such as polymorphonuclear structure of granulocyte and mononuclear feature of agranulocyte, through the employment of the reduced nicotinamide adenine dinucleotide (NADH) fluorescence signals. In addition, NADH fluorescence images clearly reveal the morphological transformation process of neutrophils during disease-causing bacterial infection. Our findings also show that time-resolved NADH fluorescence can be potentially used for functional imaging of the phagocytosis of pathogens by leukocytes (neutrophils) *in vivo*. In particular, we found that free-to-bound NADH ratios measured in infected neutrophils increased significantly, which is consistent with a previous study that the energy consumed in the phagocytosis of neutrophils is mainly generated through the glycolysis pathway that leads to the accumulation of free NADH. Future work will focus on further developing and applying label-free imaging technology to investigate leukocyte-related diseases and disorders. [DOI: 10.1117/1.JBO.18.4.040103]

Keywords: human leukocyte; two-photon excited endogenous fluorescence imaging; reduced nicotinamide adenine dinucleotide; bacterial infection; fluorescence lifetime.

Paper 12697LRR received Oct. 25, 2012; revised manuscript received Feb. 27, 2013; accepted for publication Mar. 8, 2013; published online Apr. 2, 2013.

Leukocytes are cells of the immune system, engaged in a variety of biological processes related to significant organ disorders and diseases, such as inflammation, cancer, diabetes, atherosclerosis, acquired immune-deficiency syndrome, etc.[1,2] *In vivo* imaging provides unique information to study and understand the functional roles of leukocytes in immunity promotion and disease prevention. Fluorescent dyes and fluorescent proteins have been used to track the dynamic activities of targeted leukocytes.[3,4] However, it is biologically challenging to translate label-based technology for applications in high-level animals and humans. To achieve label-free imaging of leukocytes noninvasively, reflectance confocal microscopy, two-photon excited fluorescence (TPEF) imaging, and third harmonic generation microscopy have been developed recently to visualize the rolling and adherent leukocytes in biological tissue *in vivo*.[5–7]

Our recent study discovered that NADH TPEF signals provide intrinsic contrast for *in vivo* imaging of neutrophil trafficking in zebrafish vascular vessels.[8] The results encourage morphological and functional imaging of diverse leukocyte activities *in vivo* using cellular NADH TPEF signals. In addition, NADH fluorescence lifetime provides a method to discriminate between the statuses of NADH molecules (free or bound to protein).[9] In this work, we characterize various types of human blood cells (erythrocytes, granulocytes, agranulocytes, and platelets) using endogenous TPEF signals. Specifically, the NADH TPEF signals provide excellent morphological contrast for imaging human leukocytes. Using spectral and time-resolved TPEF imaging, we study the phagocytosis of pathogens by neutrophils, a major component of leukocytes. We demonstrate that TPEF imaging can potentially provide both morphological and biochemical information for *in vivo* and real-time monitoring of the functional dynamics of leukocytes in the immune responses to disease-causing bacterial infection.

Experimentally, an inverted two-photon spectroscopic lifetime fluorescence imaging system was modified from the previously reported upright system.[8] To avoid any cell damage and photobleaching, the excitation power of different excitation wavelengths was kept at not over 10 mW on the samples.[10] Three major components of blood (erythrocytes, granulocytes, and agranulocytes with platelets) were isolated from human blood by Ficoll-Histopaque density gradient centrifugation following the standard protocol (Sigma-Aldrich). The granulocytes were further purified by excluding the contamination of erythrocytes using a red blood cell lysis buffer. All of the reagents used in the experiment were bought form Sigma-Aldrich. The Discosoma sp. red fluorescent protein (DsRed) labeled gram-negative *Escherichia coli* (*E. coli*) strain DH5α (containing pDSK-DsRed plasmid) was prepared in the same way as previously reported.[11] *E. coli* without opsonization was harvested by centrifugation and the pellet of the bacteria was resuspended in Roswell Park Memorial Institute (RPMI) 1640 medium and stored under 37°C for the experiment on bacterial infection. The fluorescence measurement for each sample was finished within 10 min at room temperature.

We first conducted TPEF measurement at different excitation wavelengths for various blood cells suspended in a phosphate buffer saline. The TPEF images of isolated blood components excited at 600 nm are shown in Fig. 1(a) to 1(c), and the images of excitation at 720 nm are shown in Fig. 1(d) to 1(f). The spectra shown in Fig. 1(g) and 1(h) confirmed that the TPEF signals of leukocytes excited at 600 nm and 720 nm were from tryptophan fluorescence peaked at 350 nm and NADH fluorescence peaked at 445 nm, respectively.[12] At 600-nm excitation, relatively homogenous round patterns were found in the images

Address all correspondence to: Jianan Y. Qu, Hong Kong University of Science and Technology, Department of Electronic and Computer Engineering, Biophotonics Research Laboratory, Clear Water Bay, Kowloon, Hong Kong SAR, China. Tel: +(852) 2358-8541; Fax: +(852) 2358-1485; E-mail: eequ@ust.hk

0091-3286/2013/$25.00 © 2013 SPIE

of resting granulocytes (10 to 12 um) and agranulocytes (7 to 8 um), as shown in Fig. 1(a) and 1(b). However, the subcellular structures could not be clearly revealed. This may be due to the fact that tryptophan is a basic building block of protein and the protein distribution is relatively uniform across the leukocyte body.[6] In contrast, with an excitation at 720 nm, a wavelength favoring NADH fluorescence excitation, the structural differences between granulocytes and agranulocytes could be clearly identified. As displayed in Fig. 1(d), the NADH TPEF signals produced excellent contrast to allow visualization of the distinct polymorphonuclear lobe's feature of the granulocytes (dark round feature inside the cell body), which was confirmed by the Wright-Giemsa stain of the granulocytes (95% are neutrophils), as shown in the enlarged bright field image of Fig. 1(d). In addition, we found that the NADH signals were relatively uniformly distributed in cytoplasm and the bright, thread-shaped mitochondria of highly concentrated NADH were not clearly identified in neutrophils. This finding is consistent with the well-known fact that ATP synthesis in neutrophils mainly takes place in cytosol through glycolysis, rather than in mitochondria through oxidative phosphorylation.[13] On the other hand, the NADH signal distribution in the image of the agranulocytes is highly heterogeneous. As shown in Fig. 1(e), because the NADH signals from thread-shaped mitochondria were dominant, we set the gamma value of the image to 0.6 to visualize other cellular structures at a much lower signal level. We also discovered small spots of 2 to 3 um, as pointed out by white arrows in Fig. 1(b) and 1(e). The blood smear in Fig. 1(e) identified that these small features were platelets. As shown in Fig. 1(g) and 1(h), the spectral analysis of the signals from the small spots confirmed that the endogenous fluorescence of the platelets was also from the tryptophan signal at 600-nm excitation and the NADH signal at 720-nm excitation. Finally, the erythrocytes, shown in Fig. 1(c) and 1(f), were clearly visualized based on their strong hemoglobin fluorescence.[14]

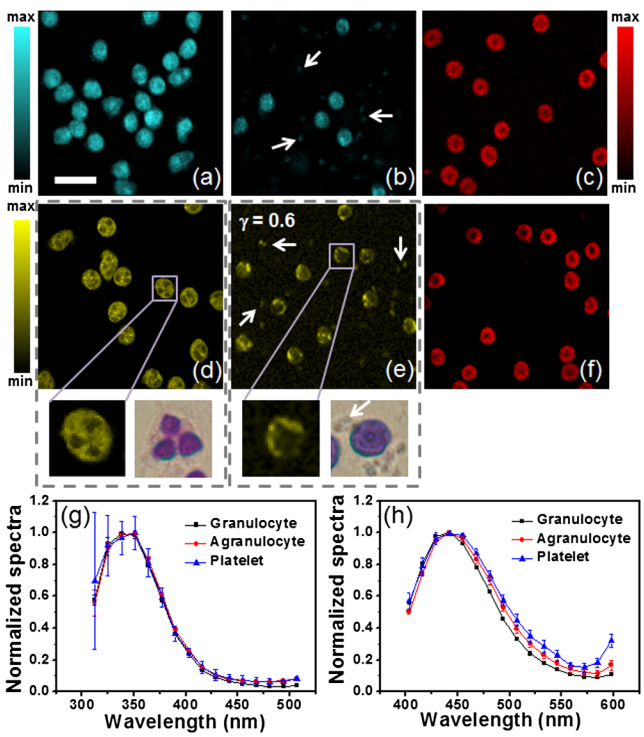

Fig. 1 Fluorescence characteristics of human blood cells. (a) through (c) TPEF images of granulocytes, agranulocytes with platelets, and erythrocytes under 600 nm excitation; (d) through (f) TPEF images of granulocytes, agranulocytes with platelets, and erythrocytes under 720 nm excitation. The bright field images shown in (d) and (e) are blood smears of granulocytes and agranulocytes with platelets; (g) and (h) Normalized spectra of blood cell autofluorescence under 600 nm (5 mW) and 720 nm (10 mW) excitation, respectively. The acquisition time for each TPEF image: 32 s; resolution: 128 × 128 pixels; scale bar: 20 μm; γ is the gamma value in the gamma correction of (e).

Since NADH fluorescence is a known indicator of cellular metabolism, its fluorescence can be potentially used to measure biochemical changes when leukocytes track down and destroy pathogens. In our work, we studied the immune response of neutrophils (the first line of defense against bacterial infection) to DsRed-labeled *E. coli*. The process for simulating bacterial infection was to uniformly mix neutrophils and *E. coli* in RPMI 1640 medium.[15] Here, DsRed fluorescence, efficiently excited at 720 nm due to the two-photon resonance absorption, [16] was used to localize *E. coli* in the mixture. Figure 2(a) and 2(c) shows the TPEF images of resting control neutrophil samples (regular round shapes) formed with the NADH signal in the band from 400 to 530 nm. After 45 and 90 min of mixing neutrophils and *E. coli*, infected neutrophils of ruffle shapes with membrane protrusions could be identified from the merged TPEF images, as shown in Fig. 2(b) and 2(d) where the NADH fluorescence band (400 to 530 nm) is color-coded in yellow and the DsRed fluorescence band (550 to 600 nm) is coded in red. The distinct phagosomes (dark circles) inside the neutrophils were also visualized, indicating that NADH cannot freely diffuse through the phagosome membrane. The TPEF images also showed that the *E. coli* bodies were inside the phagosomes, which normally contain a large amount of reactive oxygen species and antimicrobial cytotoxic molecules for destroying bacteria.

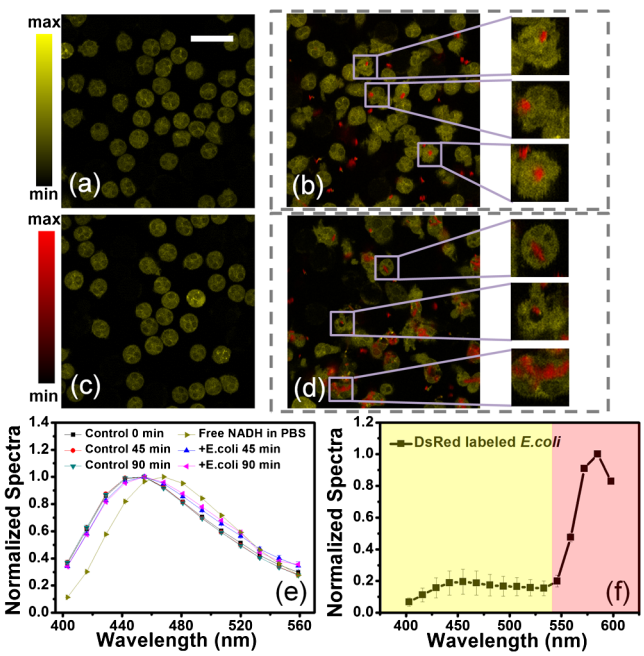

Fig. 2 Two-photon excited fluorescence images of bacterial infection (DsRed-labeled *E. coli*) with neutrophils. (a) and (b) NADH TPEF images of control and *E. coli*-infected neutrophils at 45 min; (c) and (d) NADH TPEF images of control and *E. coli*-infected neutrophils at 90 min; (e) TPEF spectra of neutrophils; (f) TPEF spectra of DsRed-labeled *E. coli*. The acquisition time for each TPEF image: 32 s; resolution: 512 × 512 pixels; scale bar: 20 μm.

Table 1 A_1/A_2 ratio and lifetimes measured from neutrophil and *E.coli*.[a,b]

Time (min)		0 min	45 min	90 min
Resting neutrophil	A_1/A_2	4.11 ± 0.28	4.12 ± 0.31	4.23 ± 0.31
	τ_1	0.46 ± 0.02	0.45 ± 0.02	0.45 ± 0.02
	τ_2	3.36 ± 0.12	3.25 ± 0.16	3.36 ± 0.23
Neutrophil (+*E.coli*)	A_1/A_2		5.34 ± 0.28	5.45 ± 0.33
	τ_1		0.40 ± 0.02	0.41 ± 0.02
	τ_2		2.94 ± 0.19	2.88 ± 0.12

[a]Ratios and lifetimes are calculated within the wavelength band of 430 to 460 nm, where NADH fluorescence is peaked.
[b]The values of all parameters are shown in terms of the average (with standard deviation) over five measurements.

Next, we analyzed the TPEF spectra of neutrophils infected by *E. coli* and studied the biochemical changes during phagocytosis. An imaging-guided spectroscopy method was used to obtain pure TPEF signals from the infected neutrophils and *E. coli*.[17] For example, we summed up the signals from the pixels of neutrophils and excluded the pixels containing DsRed fluorescence signals. The TPEF signals from neutrophils and *E. coli* are shown in Fig. 2(e) and 2(f), respectively. As can be seen in Fig. 2(e), the NADH fluorescence spectra of the resting neutrophils were kept unchanged at the three measured time points (0, 45, 90 min), while a small red-shift (but difficult to identify) of the NADH fluorescence spectra of the infected neutrophils was observed. This may be due to the increased ratio of free-over-bound NADH because the free NADH fluorescence peak is located at a longer wavelength than that of protein-bound NADH, as displayed in Fig. 2(e).[17] To further study the change in the ratio of free-over-bound NADH, we analyzed the lifetime of the summed-up TPEF signals utilizing a dual exponential decay model: $A_1 \cdot \exp(-t/\tau_1) + A_2 \cdot \exp(-t/\tau_2)$. Two lifetime components, A_1 and A_2, represent the relative contributions of the free NADH and protein-bound NADH while τ_1 and τ_2 are the short- and long-lifetime components, respectively. The results are summarized in Table 1. We found that the free-to-bound NADH ratios (A_1/A_2) measured in infected neutrophils increased significantly in comparison with the control samples, which indicated an increase of the free NADH and explained the small red-shift of the NADH fluorescence. This is consistent with a previous study that the energy consumed in the phagocytosis of neutrophils is mainly generated through the glycolysis pathway that leads to the accumulation of free NADH.[13] We also noted that the short lifetime (τ_1) representing free NADH remained unchanged (~0.4 ns) while the long lifetime (τ_2) dropped significantly from 3.36 to 2.88 ns after 90 min exposure to bacteria ($p < 0.01$). The alteration in the long lifetime may be associated with the change of binding sites profile or interference from increased short-lifetime free NADH fluorescence.[17]

Finally, it should be emphasized that about one third of the total NADH fluorescence signals of neutrophils are contributed from NADPH, the phosphate form of NAD with similar fluorescence characteristics to NADH.[18,19] During bacterial infection, NADPH is consumed by NADPH oxidase to generate oxidative species to destroy bacteria. To maintain the necessary NADPH pool for immune function, synthesis of new NADPH takes place through a hexose monophosphate shunt pathway. Biochemical studies have indicated that the concentration of NADPH in neutrophils decreases during phagocytosis.[18,20] Therefore, the increased free-to-bound NADH ratio measured in infected neutrophils may be underestimated due to the decrease in NADPH. This work was supported by the Hong Kong Research Grants Council through grants 662711, N_HKUST631/11, T13-607/12R, and T13-706/11-1, and Hong Kong University of Science & Technology (HKUST) through grant RPC10EG33.

References

1. G. B. Pier, J. B. Lyczak, and L. M. Wetzler, Eds., *Immunology, Infection, And Immunity*, ASM press, Washington, DC (2004).
2. R. Medzhitov, "Origin and physiological roles of inflammation," *Nature* **454**(7203), 428–435 (2008).
3. S. Gross, B. L. Moss, and D. Piwnica-Worms, "Veni, vidi, vici: in vivo molecular imaging of immune response," *Immunity* **27**(4), 533–538 (2007).
4. J. L. Li and L. G. Ng, "Peeking into the secret life of neutrophils," *Immunol. Res.* **53**(1), 168–181 (2012).
5. L. Golan et al., "Noninvasive imaging of flowing blood cells using label-free spectrally encoded flow cytometry," *Biomed. Opt. Express* **3**(6), 1455–1464 (2012).
6. C. Li et al., "Imaging leukocyte trafficking in vivo with two-photon-excited endogenous tryptophan fluorescence," *Opt. Express* **18**(2), 988–999 (2010).
7. M. Rehberg et al., "Label-free 3D visualization of cellular and tissue structures in intact muscle with second and third harmonic generation microscopy," *PLoS ONE.* **6**(11), e28237 (2011).
8. Y. Zeng et al., "Label-free in vivo flow cytometry in zebrafish using two-photon autofluorescence imaging," *Opt. Lett.* **37**(13), 2490–2492 (2012).
9. M. C. Skala et al., "In vivo multiphoton microscopy of NADH and FAD redox states, fluorescence lifetimes, and cellular morphology in precancerous epithelia," *Proc. Natl. Acad. Sci. U.S.A.* **104**(49), 19494–19499 (2007).
10. L. M. Tiede and M. G. Nichols, "Photobleaching of reduced nicotinamide adenine dinucleotide and the development of highly fluorescent lesions in rat basophilic leukemia cells during multiphoton microscopy," *Photochem. Photobiol.* **82**(3), 656–664 (2006).
11. E. L. Benard et al., "Infection of zebrafish embryos with intracellular bacterial pathogens." *J. Visualized Exp.* **61**, e3781 (2012).
12. R. Richards-Kortum and E. Sevick-Muraca, "Quantitative optical spectroscopy for tissue diagnosis," *Annu. Rev. Phys. Chem.* **47**, 555–606 (1996).
13. D. J. Kominsky, E. L. Campbell, and S. P. Colgan, "Metabolic shifts in immunity and inflammation," *J. Immunol.* **184**(8), 4062–4068 (2010).
14. W. Zheng et al., "Two-photon excited hemoglobin fluorescence," *Biomed. Opt. Express.* **2**(1), 71–79 (2011).
15. A. M. Palazzolo et al., "Green fluorescent protein-expressing Escherichia coli as a selective probe for HOCl generation within neutrophils," *Biochemistry (N. Y.)* **44**(18), 6910–6919 (2005).
16. M. Drobizhev et al., "Two-photon absorption properties of fluorescent proteins," *Nat. Methods* **8**(5), 393–399 (2011).
17. D. Li, W. Zheng, and J. Y. Qu, "Time-resolved spectroscopic imaging reveals the fundamentals of cellular NADH fluorescence," *Opt. Lett.* **33**(20), 2365–2367 (2008).
18. A. Aellig et al., "The energy metabolism of the leukocyte. IX. Changes in the concentrations of the coenzymes NAD, NADH, NADP and NADPH in polymorphonuclear leukocytes during phagocytosis of Staphylococcus albus and due to the action of phospholipase C," *Enzyme* **22**(3), 207–212 (1977).
19. H. D. Vishwasrao et al., "Conformational dependence of intracellular NADH on metabolic state revealed by associated fluorescence anisotropy," *J. Biol. Chem.* **280**(26), 25119–25126 (2005).
20. R. J. Selvaraj and A. J. Sbarra, "The role of the phagocyte in host-parasite interactions. VII. Di- and triphosphorydine nucleotide kinetics during phagocytosis," *BBA—General Subjects* **141**(2), 243–249 (1967).